A Lagrangian View of Stratospheric Trace Gas Distributions

M. R. Schoeberl
NASA Goddard Space Flight Center, Greenbelt, MD

L. Sparling and A. Dessler
University of Maryland
College Park and Baltimore, MD.

C. H. Jackman
NASA Goddard Space Flight Center, Greenbelt, MD

and

E. L. Fleming
Raytheon-STX
Laurel, MD.

Abstract

As a result of photochemistry, some relationship between the stratospheric age-of-air and the amount of tracer contained within an air sample is expected. The existence of such a relationship allows inferences about transport history to be made from observations of chemical tracers. This paper lays down the conceptual foundations for the relationship between age and tracer amount, developed within a Lagrangian framework. In general, the photochemical loss depends not only on the age of the parcel but also on its path. We show that under the "average path approximation" that the path variations are less important than parcel age. The average path approximation then allows us to develop a formal relationship between the age spectrum and the tracer spectrum. Using the relation between the tracer and age spectra, tracer-tracer correlations can be interpreted as resulting from mixing which connects parts of the single path photochemistry curve, which is formed purely from the action of photochemistry on an irreducible parcel. This geometric interpretation of mixing gives rise to constraints on trace gas correlations, and explains why

some observations are do not fall on rapid mixing curves. This effect is seen in the ATMOS observations.

1. Introduction

As air enters the tropical stratosphere, it moves upwards and towards the extra tropics roughly along the streamlines of the Brewer-Dobson circulation. Mass balance requires that most of the air rising into the tropical stratosphere will immediately move poleward and subsequently descend into the middle world (see Holton et al., 1995 for discussion of the middle world region of the stratosphere). However, some air continues to rise into the stratosphere and mix with the environment. Understanding the movement, residence time and mixing of air within the stratosphere is key to assessing the impact of pollutants on the ozone layer.

The measurement of nearly inert trace gases, which have known time-dependent sources, can be used to estimate the time elapsed since the air first entered the stratosphere. This transit time is commonly called the age-of-air, and it gives important clues about the stratospheric circulation. The age-of-air depends not only on the time scale of the mean circulation, but also on fluctuations around the mean transport; that is, it depends on the mixing. As we discuss below, the sampled air can have a complex time history, thus the transit time from the tropopause to some point within the stratosphere is not in general well-characterized by a single time scale.

The realization that the character of a sample of air is determined by both the transport and mixing history has led to the idea that the transit time is more aptly described by a distribution of time scales [Kida, 1983; Hall and Plumb, 1994]. In this distribution, each element corresponds to a single path connecting the source and observation or sample point. Thus, an air sample can be considered to consist of a large number of "irreducible parcels," each of which has traveled along a single path that has wandered into the

observation region at the time of the measurement. There are of course a very large number of such paths, the maximum number being the number of molecules in the sample. One need not consider such a large number, however, the number of paths need only be chosen sufficiently large so that all the relevant ensemble statistics have converged. Increasing the number of parcels beyond this point will introduce nothing new. Thus, the sample consists of a statistically robust ensemble of "irreducible parcels" which have taken different paths to the sampling volume. The term parcel will here after refer to an irreducible parcel.

In terms of such an ensemble of paths, the age-of-air can then be interpreted as the mean of the transit time distribution, commonly referred to as the "age spectrum" [Hall and Plumb, 1994] (hereafter HP). Although it is easy to compute the age spectrum for a numerical model for which the mixing history is known, it is not possible to infer the age spectrum solely from observations. Given only an observation of the total amount of trace gas in the sample, we have no a priori knowledge of its detailed time history. Under some conditions however, the mean age of a sample can be inferred from the amount of trace gas in the sample. This becomes possible when there is something in the system that acts as a "clock", marking the passage of time along a parcel path from the source to the observation point. One example is an inert tracer with a monotonically increasing source $S(t)$ [HP]. In this case, a parcel entering the stratosphere at time, T, has mixing ratio $S(T)$, and is therefore tagged by its entry time.

Another example of a stratospheric clock occurs when the source is constant in time, but the amount of trace gas in the parcel decays with time. In the simplest case, the decay rate is independent of ambient conditions and is thus independent of path, for example a radioactive tracer. In this simple situation, two parcels that take the same time to travel from the source to the observation point will have the same amount of tracer, even if they have traveled on different paths. This means that there is a 1:1 correspondence between the

amount of trace gas in the parcel and the age of the parcel. The actual amount of a constituent measured in the sample is the volumetric average of the trace gas amounts of all parcels comprising the sample. Because there is a distribution of ages in the sample, there will also be a distribution of photochemical losses and by analogy to the age spectrum, the probability distribution function (PDF) of the ratio of the trace gas amount to its stratospheric entry value is the tracer spectrum.

In the case of stratospheric tracers such as N_2O or CH_4, the situation is more complicated. The amount of photochemical loss now depends on the accumulated exposure to sufficiently high-energy photons or locally generated radicals. For such "total exposure constituents" [McIntyre, 1990], the 1:1 relation between age and trace gas amount is blurred, and parcels with the same age may have different trace gas amounts, depending on the latitude and altitude range of their paths. This problem is illustrated in Figure 1. The cartoon shows two parcels that have the same age although they take different paths to arrive at the sample point with different N_2O amounts. This cartoon also illustrates the Lagrangian view of the mixing and transport process. The "sample" is the local assembly of irreducible parcels that have taken many different paths to the sample region. Because the parcels are irreducible, by definition, the parcels do not mix with their environment on the way to the sample point.

As mentioned above, although we cannot directly observe the age spectrum in the real atmosphere, the age spectrum can be computed for a model. There are two methods. The first method is an Eulerian calculation. A pulse of inert tracer is released at the tropopause and allowed to disperse throughout the stratosphere. At a given point within the model domain, the graph of the tracer amount versus time gives the age spectrum. Computing the age spectrum in this way is equivalent to finding the Green's function solution to the model transport dynamics [HP], and assumes that non-stationary processes are negligible on the

multi-year time scale of the problem. Hall and Waugh [1997] report the age spectrum and age-of-air distributions for two general circulation models using this method.

The second method is Lagrangian. A diabatic or kinematic trajectory model is used to move a large number of air parcels that are continuously released at the tropopause. After a long time (years), the age spectrum for a sample volume containing many parcels can be computed. No assumptions of stationarity are made, which means that a trajectory computed age spectrum will vary in time. A further advantage of the trajectory method is the fact that Eulerian estimates of the age-of-air appear to depend on the advection scheme [Eluszkiewicz, personal communication] while the trajectory transport is non-dispersive. The disadvantage of the trajectory method is that a very large number of parcels need to be used because the parcel density, like the atmospheric number density, decreases exponentially with altitude.

The trajectory model method has an advantage in that it allows us to develop a Lagrangian interpretation of mixing and transport. For example, the observation that long-lived tracers are highly correlated producing a compact relationship has become an important tool in interpretation of stratospheric data. The formation of such a compact relationship is explained in a seminal paper by Plumb and Ko [1992] (hereafter PK). But how do such compact tracer-tracer correlations develop from a Lagrangian viewpoint? A main goal of this paper is to demonstrate how tracer-tracer correlations can be understood within a Lagrangian framework.

In the next section, we develop the approximations that us to relate the tracer and age spectra. We use some analytical and numerical examples to illustrate our concepts and test the methodology. In Section 3, we extend the formalism to tracer-tracer correlations and

show how such correlations can be interpreted within a Lagrangian framework. The last section summarizes the paper.

2.0 Photochemistry along Lagrangian paths

Following Kida [1983], Plumb and McConalogue [1988], HP, and Hall and Waugh [1997], we postulate, as discussed above, that a "sample" of air contains a large number of irreducible parcels with different ages and composition. In the Lagrangian view, each of these irreducible parcels has traveled from the tropical tropopause (where we assume that all air enters the stratosphere) to a sample point as illustrated in Figure 1. Since these are irreducible parcels, mixing does not take place along the paths, but is implied in the formation of the sample. The dependence of the total photochemical exposure on the parcel path gives rise to a distribution of trace gas amounts in the ensemble. In the following we establish that an approximate relation between the tracer and age distributions exists. That is, parcels with similar ages have similar photochemical exposures. This approximation allows us, in principle, to use photochemically active trace gases as markers of age.

The age spectrum $G_o(T, \vec{x}_s, \vec{x}_o)dT$ is the probability that the transit time from the source at $\vec{x}_o$ to the sample point $\vec{x}_s$ is in the range T to $T+dT$, $\int_0^\infty G_o(T, \vec{x}_s, \vec{x}_o)dT = 1$. We identify $G_o(T, \vec{x}, \vec{x}_o)$ as the Green's function for an inert tracer with a source $B_o(T, \vec{x}_o)$ at $\vec{x}_o$ such that $B_s(\vec{x}_s, \vec{x}_o) = \int_0^\infty B_o(T, \vec{x}_o)G_o(T, \vec{x}_s, \vec{x}_o)dT$. The sample mean age, or age-of-air, $\Gamma_s = \int_0^\infty G_o(T, \vec{x}_s, \vec{x}_o)TdT$ [HP]. For inert tracers with known time dependent sources, the age-of-air and the constituent amounts are directly related. With a linearly increasing inert tracer source, such as SF_6 or CO_2, $B_o(T, \vec{x}_o) \sim T$. Thus, it is immediately obvious that the SF_6 or CO_2 amount will be proportional to the age-of-air (e.g. Bischof et al., 1985;

Schmidt and Khedim, 1991; Boering et al., 1996, for CO_2; Elkins et al., 1996; Harnish et al., 1966; Patra et al., 1997, for SF_6).

Now we consider the case of a photochemically active tracer with a fixed tropopause mixing ratio. As mentioned earlier, the amount of tracer in each irreducible parcel depends on the path the irreducible parcels take to the sample point. Thus two parcels with the same age having different paths will very likely have different photochemical histories.

We assume all air parcels are released at the tropical tropopause with constituent mixing ratio B_o which we take to be unity. The parcel follows path $\bar{x}_i(t)$ and has a chemical loss rate $\beta(\bar{x}_i(t),t)$ The parcel amount of B_i is given by

$$\frac{DB_i}{Dt} = -\beta(\bar{x}_i(T),T)B_i \tag{1}$$

where D indicates a Lagrangian (along path) derivative. Integrating (1) over the time, T, (the parcel age) it takes the parcel to arrive at the sample point, we obtain

$$log(B_i) = -\int_0^T \beta(\bar{x}(T),T)dT = -T_i\bar{\beta}_i(T_i) \tag{2}$$

where $\bar{\beta}_i(T) = \frac{1}{T_i}\int_0^{T_i} \beta(\bar{x}_i(T),T)dT$ and where the integration is over the i'th parcel path. The overbar indicates the average over a single path. Let $P(B_i)$ be the distribution of tracer amounts within the sample. By analogy with the age spectrum, we define the tracer spectrum $P(B_i)$ such that

$$B_s = \int_0^1 P(B_i)B_i dB_i \tag{3}$$

We define

$$P(B_i) = \int_0^\infty P(B_i, \vec{x}_s, \vec{x}_o \mid T) G_o(T, \vec{x}_s, \vec{x}_o) dT \tag{4}$$

where $P(B_i, \vec{x}_s, \vec{x}_o \mid T)$ is the conditional probability distribution of tracer amounts over the subset of irreducible parcels that have arrived at the sample point $\vec{x}_s$ at time T. To simplify the notation we now suppress the explicit space dependence on the location of the sample point.

2.1 Radioactive tracer

We first consider the simple example of a radioactive tracer which has a path independent photochemical loss and is released at the tropopause. For this tracer, $\beta_i = \beta$ = a constant, and the loss along the path is simply $B_i = e^{-\beta T}$. Since there is now a one to one relation between B_i and T

$$P(B_i \mid T) = \delta(B_i - e^{-\beta T}) \tag{5}$$

Substituting (5) into (4) gives

$$P(B_i) = \int_0^\infty \delta(B_i - e^{-\beta T}) G_o(T) dT = \frac{1}{\beta B_i} G_o(-log(B_i)^{1/\beta}) \tag{6}$$

Equation (3) can be written as

$$B_s = \int_0^\infty G_o(T) e^{-\beta T} dT \equiv \tilde{G}_o(\beta) \tag{7}$$

where $\tilde{G}_o(\beta)$ is the Laplace transform of the age spectrum.

Let us now consider an actual example using the analytic age spectrum from the 1-D diffusion model as developed by HP. The HP age spectrum is given by

$$G_o(z,T) = \frac{z}{2\sqrt{\pi K T^3}} exp(-(z/\sqrt{4KT} - \sqrt{KT}/2H)^2), \tag{8}$$

where K is the diffusion coefficient, H is the atmospheric scale height, and z is the height. Despite its simplicity, this age spectrum (Eq. 8) has many characteristics of more realistic age spectra produced by 3D and 2D transport models. The Laplace transform of Eq. (8) is

$$\tilde{G}_o(\beta, z) = exp(\frac{z}{2H} - \frac{z}{2H}\sqrt{1 + 4\beta H^2/K}) \tag{9}$$

Figure 2 shows the age spectrum and four corresponding tracer spectra, $P(B)$, for different values of β using Eq. (9). For short-lived tracers, the tracer spectrum is quite broad reflecting the spread in tracer values within the sample due to photochemistry. For very fast photochemistry, a large number of parcels have zero tracer content and the distribution "piles up" on the left-hand side of the figure. On the other hand, for an inert tracer, the tracer spectrum is a δ-function on the right hand side, $\delta(B_s - B_o)$.

For long lived tracers, $4\beta H^2/K << 1$, then (9) becomes

$$B_s \approx exp(-z\beta H/K) = exp(-\beta\Gamma),$$

$$\text{or } \Gamma = -log(B_s)/\beta, \tag{10}$$

as might be expected. (Note that the quantity $4H^2/K \approx 2$ years for $K = 3.1m^2/s$ [HP], $H = 7km$ as used in Fig. 2.)

Sometimes a supposedly inert tracer is found to have a weak photochemical loss [e.g. Hall and Waugh, 1998]. The effect of this photochemistry is to shift the estimated age-of-air toward younger values. To show this, let Γ_β be the apparent age-of-air derived from non-inert tracer, then

$$\Gamma_\beta = \int_0^\infty G_o e^{-\beta T} T dT/\tilde{G}_o = -\frac{\partial}{\partial\beta} log(\tilde{G}_o). \tag{11}$$

Substituting (9) into (11) we obtain

$$\Gamma_\beta = \frac{zH}{K}(1 + 4\beta H^2/K)^{-\frac{1}{2}} \tag{12}$$

Clearly, $\Gamma_\beta \leq \Gamma$ for all positive values of β and in the limit that β goes to zero, (12) reproduces HP's result, $\Gamma_\beta = \Gamma = zH/K$, and for $\beta << K/H^2$,

$$\Gamma_\beta = \Gamma(1 - 2\beta H^2/K + ...). \tag{13}$$

If a nearly inert tracer is used to estimate the age of air, Eq. (12) gives the correction factor for chemistry.

2.2 Photochemically active tracers

For most trace gases of interest, the loss rate is not constant so the relation between the age spectrum to the tracer spectrum is not straightforward. However, Eqs. (3) and (4) can be generalized to include photochemical processes that are path dependent. Although, the time dependence is not explicitly included in the derivation below, the effects of time dependence on the photochemical loss rates will assumed to be small because the integration over long paths effectively integrates over seasonal variations in photochemical loss.

From (2), (3) and (4),

$$B_s = \int_0^\infty G_o(T) < e^{-\bar{\beta}_i(T)dT} > dT \tag{14}$$

where $< e^{-\bar{\beta}_i(T)T} >= \int_0^1 B_i P(B_i \mid T) dB_i$ and <> indicates the ensemble average over all paths of age T.

Now assume that there is an ensemble average photochemical loss rate for a given age value, and that the deviations from ensemble average loss rate are small. Thus, we assume that $\bar{\beta}_i =< \bar{\beta}(T) > + \overline{\delta\beta}_i(T)$ where $< \overline{\delta\beta}_i(T) >= 0$ and $\frac{\overline{\delta\beta}_i(T)}{< \bar{\beta} >} << 1$. Then,

$$\int_0^\infty G(T) < e^{-\bar{\beta}_i T} > dT = \int_0^\infty G(T) e^{-<\bar{\beta}_i>T} < e^{-\delta\beta_i T} > dT$$

$$= \int_0^\infty G(T) e^{-<\bar{\beta}_i>T} < 1 - \delta\beta_i T + (\delta\beta_i T)^2/2 ... > dT \tag{15}$$

The second term in the Taylor expansion vanishes identically, and we note that most of the contribution to the integral comes from times $T \leq 1/<\overline{\beta}>$ so that for large T's the higher order terms vanish. Thus

$$B_s = \int G e^{-<\overline{\beta(T)}>T} dT \tag{16a}$$

To summarize, we are essentially saying that

$$< e^{-\overline{\beta}_i T} >= e^{-<\overline{\beta}>T}. \tag{16b}$$

As we shall show below, (16) turns out to be a good approximation for most long lived trace gases with tropospheric sources. For parcels with high age values, we have found that there is a much greater dispersion in photochemical exposure so δ can be quite large; however, for these older parcels photochemistry reduces the constituent amounts so much that variations in photochemical exposure are irrelevant. Thus the truncation of the Taylor expansion in (15) appears justified. Eq (16) allows us to make the same direct connection between the age spectrum and the tracer PDF we exploited in the case of the radioactive tracer.

We now turn to the problem of computing $<\overline{\beta}(T)>$. To the same order of approximation, $<\overline{\beta}(T)>=\beta(<\bar{x}(T)>)$ where $<\bar{x}(T)>$ is the average path of duration T from the source position $\bar{x}_o$ to the sample position $\bar{x}_s$. The "average path approximation" or APA works because the variability in photochemical loss is usually not a strong function of meridional position (see Fig. 1). Even when the meridional variation of photochemical loss is large, such as across the polar vortex, the meridional parcel excursions are small.

2.3 Numerical model

To further explore the theoretical model and approximations developed above we use a 2-D trajectory model which utilizes the residual circulation and mixing coefficients of the 2-D chemical model of Jackman et al. [1996]. The residual circulation is computed from diabatic heating rates. To simulate mixing, we scramble the vertical and horizontal parcel positions at each time step by length, $L = R\sqrt{K\Delta t}$ where R is a random number which takes on the values of -1 or 1 [Feller, 1968]. K is K_{yy} or K_{zz}, in the usual notation. We tested this procedure by computing K_{yy} from the parcel dispersion using $K_{yy} = \frac{1}{2}\frac{\partial < y^2 >}{\partial t}$ where y is N-S distance [Kida, 1983] and confirming that the diagnosed K_{yy} was equal to the 2D model K_{yy}.

The advantage of using the 2-D trajectory model compared to a 3-D trajectory model is that the faster interpolation and lower memory requirements of the 2-D model permit fast multi-year integration for a very large number of parcels. The 2-D trajectory model is about 100 times faster than the 3-D model. The age-of-air distribution for the 2-D model [Fleming et al., 1998] agrees reasonably well with aircraft observations reported by Waugh et al. [1997b], and parcel spectra from long runs of a 3D trajectory model are very similar to the spectra from the 2-D model.

Figure 3a shows model back trajectories for 2001 parcels uniformly placed in a 1 degree latitude by 1 km altitude sample domain at 35°S and 30 km. Parcels are integrated backward for 10 years. The parcel age is defined here as the time it takes for a parcel to move on a backward trajectory from the sample point to below 2 km in altitude. In Figure 3a, parcel position points along each path are plotted every 3.6 days down to 10 km altitude; the average path for all the parcels is also shown as the thick white line. The average path is

computed by averaging all parcel x and y positions at each backward step down to the tropical tropopause. The figure shows that most parcels are near the average path although there are some wide excursions for the oldest parcels.

The age PDF for the calculation shown in Figure 3a is shown in Figure 3b. The minimum age of any parcel is about two years. Starting after 2 years, the age PDF generally resembles the age spectrum for the HP diffusion model (Eq. 8) as well as the age spectra for most 3D and 2D models [Waugh et al., 1997b, Hall et al., 1998].

As an aside, it is interesting to compare the age-of-air for the 2D model using the Lagrangian and Eulerian methods. This comparison provides a further check on the quality of the trajectory calculations. Figure 4a shows the 2-D model age-of-air computed using the Eulerian method. Figures 4b,c show the January 1, Lagrangian computed age-of-air with and without mixing, respectively. The Lagrangian calculation with mixing is performed using 1° by 1 km, sample regions (like that shown in Figure 3, see also Figure 6a) located on the 2-D model grid points. From each of the sample regions, 400 parcels were run backward for 20 years. To show the effect of mixing on the age-of-air, the parcel calculation shown in Fig. 4b is rerun with $K_{yy} = K_{zz} = 0$ above 10 km. If there is no mixing, the age spectrum for each sample box is very narrowly peaked. (It is not a delta function because there is mixing within the troposphere.). We thus were able to estimate the age-of-air using a uniform 2 km by 2° grid of sample boxes containing only a few parcels per sample box. This grid resolution is much higher than the 2-D model grid. The results of the no-mixing experiment are shown in Figure 4c.

Although the age-of-air distributions shown in Figs. 4a and 4b are in general agreement, there are some interesting and not completely explained differences between the trajectory age-of-air calculation and the Eulerian age-of-air calculation. For example, the Eulerian

calculation shows older air at high latitudes and altitudes compared the trajectory-computed age. We have not found an explanation for this difference, although it is probably due to the Eulerian transport scheme.

The trajectory age-of-air calculation also shows more descent at the South Pole than at the North Pole which is opposite to the Eulerian computed age-of-air. This difference arises from the fact that the Eulerian method averages over seasonal fluctuations in transport, while the trajectory method produces an instantaneous age-of-air distribution for January 1. The trajectory model is exhibiting the remains of the strong south polar descent of old air from the upper stratosphere while the Eulerian calculation shows the seasonal average of descent over both poles. We also note that the tropical zone of young air is quite narrow in the Fig. 4a, but is comparatively broad on the northward tropical flank in Fig 4b. This is also characteristic of a seasonal effect. The calculation shown in Figure 4c gives similar results to Figure 4b except that the air outside the tropical lower stratosphere is everywhere younger than that shown in Fig.4b. The increase in age-of-air from 4b to 4c occurs because that path lengths are always longer when random walks are included.

The comparison of the age-of-air calculations is not directly relevant to this study, but it does highlight an important issue relative to Lagrangian and Eulerian transport methods, namely that Lagrangian and Eulerian transport calculations, in general, do not exactly agree. The differences between the two calculations are probably due to numerical effects associated with the Eulerian transport schemes [Eluszkiewicz, personal communication].

Using the 2D trajectory results shown in Fig. 3, we can test the approximation Eq. (16). We use the annually averaged N_2O loss rates from the 2D model and compute the N_2O amount for each parcel starting with the tropical tropopause amount as the initial condition. Figure 5a shows the scatter plot of parcel ages verses N_2O amount. There is a fairly clear

correlation between tracer amount and age (correlation coef. 0.66), but a noticeable increase in the scatter with increasing age. The increase in scatter with age results from the wider range in photochemical exposure experienced by the older parcels. Figure 5b shows the tracer spectrum and mean tracer value normalized by the tropical tropopause value. The spectrum looks similar to the tracer spectra shown in Fig. 2 for the $(5\ year)^{-1}$ loss rate, but also shows the statistical pile up at low tracer amounts seen in the short lifetime case shown in Fig. 2. The statistical pile up near zero is due to the long transit time parcels that have had high total photochemical exposure.

To test the approximation Eq. (16b) we have averaged the result. This value can be compared to the loss computed for the average path for each age bin. Figure 5c shows the average loss amount versus age (LHS of Eq. 16b) compared to the value estimated using APA (the RHS of Eq. 16b) also shown are the loss amounts for the individual parcels sorted by age. Figure 5c shows that Eq (16b) is an excellent approximation for ages up to 4 years and a reasonable approximation even for ages beyond 4 years. (There are no values below 2 years as indicated in Fig. 3b.) Figure 5d shows the original age PDF and the integrand of Eq. (16a), the modified PDF, using APA and the exact loss amounts shown if Fig. 5c. This figure shows that even though APA is less accurate for ages greater than roughly 4 years, the effect on the modified PDF is negligible because the amount of tracer is greatly reduced at large times.

Figure 6 shows the extension of the results shown in Figure 5 to the whole stratosphere. Using the annual average photochemical loss rates, the N_2O amount is computed from individual parcel trajectories and APA for each of the sample boxes shown in Figure 6a which also shows the age-of-air (same as Figure 4a). The N_2O distributions obtained using all of the trajectories and using APA are shown in Figs. 6a and 6b, respectively. In general the differences between exact and APA are small, consistent with the results we

expect from in Fig. 5d. Closer examination (Fig. 6c) shows that exact distribution has a somewhat steeper vertical gradient with altitude than the APA computation. This is understandable since APA will tend to underestimate the contributions of longer paths. Finally, Fig. 6d shows the sample N_2O amount (for both APA and exactly computed trace gas amounts) plotted against the mean age for each of the sample boxes shown in Fig. 6a. The sample age-of-air and trace gas amount are correlated, but there is significant scatter. The scatter occurs because of variations in the age spectrum between samples with the same mean age. This result shows that mean age is not always a good predictor of the tracer amounts because the tracer amount is determined by the younger part of the age spectrum rather than whole spectrum.

3.0 Tracer-tracer correlations

Tracer-tracer correlations have emerged as one of the most important tools for unraveling physical processes within the stratosphere. The strong correlations between various long-lived tracers has been explained by Plumb and Ko (1992) (hereafter PK) as a consequence of rapid isentropic mixing combined with the large scale overturning circulation. In this section, we extend the Lagrangian approach to include tracer-tracer correlations.

Figure 7 shows a cartoon of the atmospheric sampling and analysis process. In the figure, an aircraft samples air with different ages and different tracer amounts, as indicated by the colored dots. Isochrons, or equal age isopleths, are indicated by the green contours. On a tracer-tracer diagram, the samples trace gas amounts are plotted. Each sample consists of a large number of irreducible parcels, which are characterized by the age spectrum $G(T)$. Each of the irreducible parcels contains some amount of trace gas determined by the parcel's photochemical exposure, which has reduced, in the case of Fig. 1, the trace gas from its tropopause value. The photolysis rate is $J_B = \int \sigma_B F d\lambda$ where σ_B is the

absorption cross section of B and F is the flux. Both F and σ_B are functions of the wavelength, λ. It turns out that the photolysis cross sections for many of the long-lived tracers have similar functional form [DeMore et al., 1994] so we can write $J_B = \beta_P \int \sigma F d\lambda$ where β_P is a constant. Now defining the photochemical exposure, n, where $dn = (\int \sigma F d\lambda) dT$, we can write

$$n = -log(B_i)/\beta_P \tag{17}$$

The photochemical exposure is only approximately related to actual time because of the variations in photochemical loss rates with altitude rates. We now consider a second trace gas, A, with $n = -log(A_i)/\alpha_P$. Eliminating n gives

$$A_i = B_i^{\alpha_P/\beta_P} \tag{18}$$

As parcels moves through the stratosphere, the amounts of A_i and B_i trace the "single path photochemistry curve" (SPPC) shown in Fig. 7. Even though all parcels will approximately trace the same curve, the parcels comprising the sample will end up at different spots on the SPPC. The actual tracer amount in the sample is then determined by the distribution, $G(T)$, of the irreducible parcels along the SPPC curve. The diagram at the bottom of Fig. 7 illustrates the weighting of the irreducible parcels by $G(T)$. Note that the sample points lie to the interior of the SPPC.

If the tracer photochemistry is more complex, it is easy to show that

$$log(A_i) = \int \frac{\alpha}{\beta} d(log(B_i)) \tag{19}$$

where the integration takes place over the parcel path and α is the photochemical loss coefficient for tracer A. Using (16),

$$A_s = \int_0^\infty A(T)G(T)dT = \int_0^\infty B^{<\bar{\alpha}(t)>/<\bar{\beta}(t)>}G(T)dT \qquad (20)$$

To better illustrate Eq. (20) we consider two simple examples. In the first example, the sample consists of two equal numbers of irreducible parcels that have ages T_1 and T_2. Then $G(t) = (\delta(T - T_1) + \delta(T - T_2))/2$, and $\Gamma = (T_1 + T_2)/2$, $B_s = (B_1 + B_2)/2$, and $A_s = (B_1^{\bar{\alpha}(T_1)/\bar{\beta}(T_1)} + B_2^{\bar{\alpha}(T_2)/\bar{\beta}(T_2)})/2$. The sample point (A_s, B_s) lies at the midpoint of a chord which intersects the curve at (A_1, B_1) and (A_2, B_2). In general, for a SPPC curve whose radius of curvature does not change sign over the domain, mixing will produce sample points on the interior side of the curve. All sample points must obviously lie below the chord connecting (1,1) and (0,0), the limit chord, and above the SPPC. This result can be demonstrated by considering trace gas amounts from the groups (1,1) and (0,0), and adjusting the fraction in each group continuously.

In the second example, we use the age spectrum from HP, Eq. (8). For long-lived trace radioactive trace gases, the trace gas amount is given by Eq. (9). With a little algebra it is easy to show that

$$A_s = B_s^{(1-\sqrt{1+4\alpha H^2/K})/(1-\sqrt{1+4\beta H^2/K})} \qquad (21)$$

In the limit of long-lived tracers, (21) has the same form as (18b), which recovers the result first derived by PK for the global diffuser model. In the other extreme case where the tracer is short lived, $2H\sqrt{\beta/K} >> 1$, (22) becomes, $A_s \approx B_s^{\sqrt{\alpha/\beta}}$. This function is not as curved as the SPPC because the weighting function $G(T)$ averages over the more steeply curved SPPC function thus producing a shallower curve. These results reinforce the

notion that the relationship between the tracers given by PK (their Eq. 13) applies to tracers whose lifetime is long compared to the mixing time.

To generate an even more realistic picture of tracer-tracer correlation, we use values of $\bar{\alpha}$ and $\bar{\beta}$ from the 2D model using N_2O and CFC-11 loss rates for March. In this experiment, we continuously release parcels at the tropical tropopause for 20 years and track their chemical composition. Parcels entering the troposphere are removed. At steady state, there are about 260,000 parcels in the stratosphere. The loss rates as a function of parcel age are generated using APA by sorting the trajectories by age and then averaging, $<\bar{\alpha}>= log(A_o/A)/T$, $<\bar{\beta}>= log(B_o/B)/T$ within an age bin, where A_o, B_o are tracer values at the tropopause.

Figure 8 shows linear and log plots of CFC-11 versus N_2O computed from the trajectory model. The SPPC curve shows the composition of the individual parcels. The log plot of the trace gas amounts demonstrates the prediction of an exponential form as suggested by Eq. (19). Sample trace gas values are computed using G(T) from Eq. (8). Increasing the age-of-air Γ (by increasing z in Eq.(8)) extends the age spectrum. Substituting Eq.(8) into Eq.(20) and varying z, we produce the points shown in Fig. 8 labeled with the age in years. The linear relationship between the *log(A)* and *log(B)* is predicted by Eq. (21).

Let us reverse the procedure and take the 2D chemical model global lifetimes as an estimate of $<\alpha>$ and $<\beta>$ to generate a curve from Eq. (18). The global lifetime is the ratio of the total stratospheric tracer amount to the cross tropopause tracer flux. The 2D chemical model global lifetime for N_2O is 117.8 years and for CFC-11 is 51.6 years. Using the inverse lifetimes as the loss rates, we generate the upper curve in Fig 8. This curve can be thought of as an upper bound on the mixing in the 2D model. We refer to this upper bound

as the PK-limit since Eq. (20) has the form of PK's Eq. (15) for this case. The PK-limit is below the limit chord (which is not shown, but it is a line connecting $[0,0]$ and the $[A_o, B_o]$ and above the points generated by using (20). This result suggests that the actual mixing within the 2D model produces a broader $G(T)$ value than the HP analytic model. This is not hard to imagine when we realize that there must be an age spectrum offset, as seen in Fig 3b, which is not included in Eq. (8). This offset is due to the general advection of parcels to the sample location as seen in Fig. 3a. In addition, there is large scale overturning within the 2D model, and old polar vortex air mixing with young tropical air will create a broader age spectrum than that defined by Eq. (8).

In general for a given function $G(T)$ the sample trace gas amounts must lie between the SPPC and the limit chord. The results above suggest that limit chord is not restrictive enough, and the PK-limit is probably a more realistic upper bound. The fact that mixing produces chords which connect parts of the tracer-tracer correlation curve has also been pointed out by Waugh et al. [1997] and Thuburn and McIntyre [1997] to explain mixing between discreet air masses. Here we argue further that such mixing, as characterized by the changing age spectrum as a function of season, is continuously forming and reforming points along different chords which are bounded by the SPPC.

There is clearly information about the range of mixing in the curvature of the tracer-tracer correlation. As pointed out by Holton [1986] and Mahlman et al. [1986], the stratospheric overturning circulation along with photochemistry will maintain the tracer gradients against the effect of isentropic mixing. Each isentropic level then defines a chord with a slightly different slope. This explains why even in a fairly well mixed system, the tracer-tracer correlation line will be slightly curved, and why the curve can be seen as a series of points lying on interlocking chords when the data is analyzed on isentropic surfaces as pointed out by Dessler et al. [1998].

Figure 9 shows N_2O sample values plotted against CFC-11sample values. The samples are generated by averaging the trajectory model data shown in Fig. 8 within 10° by 2 km regions. As expected, most of the model sample points fall between a line defined by the PK limit and the Lagrangian parcel curve. Overplotted on Fig. 9 are the data from the Atmospheric Laboratory for Applications and Science (ATLAS) missions 1-3 Atmospheric Trace Molecule Spectroscopy (ATMOS) instrument [Gunson et al., 1996]. The ATLAS flights took place March 24-April 3, 1992; April 8-16, 1993 and Nov. 3-14, 1994, and the ATMOS instrument acquires high-resolution infrared solar absorption spectra from which constituent profiles are retrieved. The high quality of this data set makes if useful for correlations over a wide range in CFC-11 and N_2O values. The profiles obtained by ATMOS-3 have been validated by nearby ER-2 measurements [Chang et al., 1996a,b].

The comparison between the ATMOS and 2D model data is good, although there appears to more of the ATMOS data along the PK limit line than generated using the trajectory 2D model for high values of CFC-11 and N_2O. The likely explanation for the discrepancy is a difference in the sample size between the numerical calculation and the observations. In other words, the trajectory model has not adequately characterized that age spectrum in the high N_2O - CFC-11 region due to too few parcels. For low values of N_2O and CFC-11 the size of the scatter in the ATMOS and model points is about the same and the data falls off the PK limit as older air parcels dominate $G(T)$.

4.0 Summary and Discussion

The purpose of this paper is to present a Lagrangian interpretation of the mixing of chemically active trace gases. The methodology developed extends the age-of-air formalism of HP in which a "sample" of air is defined as a collection of irreducible parcels.

The age of each of the irreducible parcels is clocked from their tropopause crossing time, andthe age spectrum is the normalized PDF of parcel ages within the sample. Because the parcels are irreducible, mixing along the parcel path does not take place, but the effects of mixing are included in the sampling of a large number of parcels. The tracer spectrum is defined as the PDF of the tracer ratio to the tracer amount at the tropopause.

Photochemical exposure, as opposed to age, is the actual clock that determines the tracer amounts for the individual parcels. For long-lived tracers, the photolysis rates are generally scalable so that there is a high degree of correlation between different trace gas amounts computed for individual parcels. On a tracer-tracer diagram, this means that the irreducible parcels form a very tight curve, which we refer to as the single path photochemistry curve (SPPC). As they move through the stratosphere, we can think of parcels moving along the SPPC. Since the sample consists of an ensemble of parcel at different points along the SPPC, the sample point must lie on the interior of the SPPC.

In order to infer transport related quantities such as mean age from trace gas measurements we must connect age and photochemical exposure. We find that the variations in photochemical exposure tend to average to zero for parcels with similar ages. Thus, for an ensemble of parcels in the sample with the same age, the photochemical exposure can be computed using the average path. This is called the average path approximation (APA). This approximation allows us to interpret the age spectrum as a "weight" which gives the relative contribution of equivalent parcels with different ages. The age spectrum can then be converted into a tracer spectrum using the photochemistry along the average path for all the parcels that have the same age. Using a 2D model, we show that these approximations work quite well for N_2O and CFC-11.

Because photochemical loss depends mainly on the parcel age, we can interpret the age spectrum as a kind of weighting function for the SPPC in the tracer-tracer correlation curve. Analytical examples which form tracer-tracer circulation curves show that these curves tend to be linear on log-log plots, a result first derived by Plumb and Ko [1992], but this is shown not to be true in general. Using the lifetime of tracers in the 2D model, we find that N_2O and CFC-11 data from the 2D model data, and from the ATMOS instrument appear to fall between the limit curves formed from the tracer lifetime limit and SPCC limit.

The extension of the age-of-air formalism to chemically trace gases allows the possibility of gaining more information on the age spectrum than can be gained from the study of inert tracers alone. Shorter-lived tracers are sensitive to younger parts of the age spectrum while the inert tracers are sensitive to the whole spectrum. The basic method would be to invert Eq. (16) given the tracer measurement and an estimate of the path integrated loss rate as a function of age. From each tracer measurement, assuming different loss rates, one new piece of information about the age spectrum would then be obtained. Because the path integrated 2D model loss rates appear to be a relatively smooth function of age and position for most long lived tracers, it may be possible to use the 2D model loss rates and actual observations to derive information about the atmospheric age spectrum.

Finally, the connection between the age and tracer spectrum suggests a strong coupling between the age-of-air diagnostic and the long-lived tracer fields. However, because the long-lived tracer distribution is not sensitive to the tail of the age spectrum while the mean age is very sensitive to the tail, the age-of-air can be a misleading diagnostic. For example, the trace gas distribution in a model might be quite unrealistic while the mean age field is very realistic and vice versa. This can happen because of the strong weight that old air parcels give to computing the mean age. At the same time the old air parcels give almost no weight to computing the tracer amount for the long lived tracers. Thus strong emphasis

should not be placed on the mean age as a diagnostic determining the success of failure of a model transport scheme especially in regions where old air parcels are a significant component of the sample (e.g. winter polar regions).

Acknowledgments

The authors would like to acknowledge helpful discussions T. Hall and D. Waugh.

4. References

Bischof, W., R. Borchers, P. Fabian, and B. C. Krueger, Increased concentration and vertical distribution of carbon dioxide in the stratosphere, Nature, 316, 708-710, 1985.

Boering, K. A., S. C. Wofsy, B. C. Daube, H. R. Schneider, M. Loewenstein and J. R. Podolske, Stratospheric transport rates and mean age distributions derived from observations of atmospheric CO_2 and N_2O, Science, 274, 1340-1343, 1996.

Chang, A. Y. et al., A comparison of measurements from ATMOS instruments aboard the ER-2 aircraft: Halogenated gases, Geophys. Res. Lett., 23, 2393-2396, 1996a.

Chang, A. Y. et al., A comparison of measurements from ATMOS instruments aboard the ER-2 aircraft: tracers of atmospheric transport, Geophys. Res. Lett., 23, 2389-2392, 1996b.

Daniel, J. S. et al., On the age of stratospheric air and inorganic chlorine and bromine release. J. Geophys. Res., 101, 16757-16770, 1996.

DeMore, W. B., et al., Chemical kinetics and photochemical data for use in stratospheric modeling, JPL Publication 94-26, 1994.

Dessler, A. et al., A generalized view of the interrelationship between abundances of long-lived trace species in the stratosphere, submitted to J. Atmos. Sci., 1998.

Elkins, J. W. et al., Airborne gas chromatograph for in situ measurements of long-lived species in the upper troposphere and lower stratosphere, Geophys. Res. Lett., 101, 16757-16770, 1996.

Feller, W., "An Introduction to Probability Theory and Its Application," Vol. 1, John Wiley and Sons, New York, 1968.

Fleming, E. L., C. H. Jackman, D. B. Considine and R. S. Stolarski, Simulation of long lived tracers using an improved empirically based two-dimensional model transport algorithm, J. Geophys. Res., in preparation, 1998.

Gunson, M. R. et al., The Atmospheric Trace Molecule Spectroscopy (ATMOS) experiment: Deployment on the ATLAS space shuttle missions, Geophys. Res. Lett., 23, 2333-2336, 1996.

Hall, T. M., and R. A. Plumb, Age as a diagnostic of stratospheric transport, J. Geophys. Res. 99, 1059-1070, 1994.

Hall, T. M., and D. W. Waugh, Timescales for the stratospheric circulation derived from tracers, J. Geophys. Res., 102, 8991-9001, 1997.

Hall, T. M., and D. W. Waugh, The influence of nonlocal chemistry on tracer distributions: inferring the mean age of air from SF_6, J. Geophys. Res., 103, 13,327-13,336, 1998.

Hall, T. M., D. W. Waugh, K. A. Boering, and R. A. Plumb, Evaluation of transport in stratospheric models, submitted to J. Geophys. Res., 1998.

Harnisch, J., R. Borchers, P. Fabian, and M. Maiss, Tropospheric trends for CF_4 and C_2F_6 since 1982 derived from SF_6 data stratospheric air, Geophys. Res. Lett., 23, 1099-1102, 1996

Holton, J. R., A dynamically based transport parameterization for one-dimensional photochemical models of the stratosphere, J. Geophys. Res., 91, 2681-2686, 1986.

Jackman, C. H., E. L. Fleming, S. Chandra, D. B. Considine, and J. E. Rosenfield, Past, present and future modeled ozone trends with comparisons to observed trends, J. Geophys. Res., 101, 28,753-28,767, 1996.

Kida, H., General circulation of air parcels and transport characteristics derived from a hemispheric GCM, Part 2, Very long-term motions of air parcels in the troposphere and stratosphere, J. Meteorol. Soc. Jpn., 61, 510-522, 1983.

Mahlman, J. D., H. Levy II, and W. J. Moxim, Three dimensional simulations for stratospheric N_2O: Predictions for other trace constituents, J. Geophys. Res., 91, 2687-2708, 1986.

McIntyre, M. E., Atmospheric Dynamics: Some fundamentals, with Observational Implications, in The Use of EOS for the Study of Atmospheric Physics, Proceedings of the International School of Physics, "Enrico Fermi" Course 115, G. Visconti and J. Gille, eds., North Holland, NY, 313-386, NATO Summer School, 1992.

Patra, P. K., S. Lal, B. H. Subbaraya, C. H. Jackman, and P. Rajaratnam, Observed vertical profile of sulfur hexafluoride (SF_6) and its atmospheric applications, Geophys. Res. Lett., 102, 8855-8859, 1997.

Plumb, R. A., A ``tropical pipe'' model of stratospheric transport, J. Geophys. Res. 101, 3957-3972, 1996.

Plumb, R. A., and M. K. W. Ko, Interrelationships between mixing ratios of long-lived stratospheric constituents, J. Geophys. Res. 97, 10,145-10,156, 1992.

Plumb, R. A. and D. D. McConalogue, On the meridional structure of long-lived tropospheric constituents, J. Geophys. Res., 97, 10145-10156, 1992.

Schmidt, U., and A. Khedim, In situ measurements of carbon dioxide in the winter arctic vortex and at midlatitudes: An indicator of the "age" of stratospheric air, Geophys. Res. Lett. 18, 763-766, 1991.

Schoeberl, M. R. and L. Sparling, Trajectory Modeling, in *Diagnostic Tools in Atmospheric Physics,* G. Fiocco and G. Visconti eds., Proceedings of the International School of Physics "Enrico Fermi", Vol. 124, 289-306,1995

Thuburn, J. and M. E. McIntyre, Numerical advection schemes, cross-isentropic random walks and correlations between chemical species, J. Geophys. Res., 6775-6796, 1997.

Waugh, D. W., et al., Mixing of polar vortex air into middle latitudes as revealed by tracer-tracer correlations, J. Geophys. Res., 102, 13119-13134, 1997a.

Waugh, D. W., et al., Three dimensional simulations of long lived tracers using winds from MACCM2, J. Geophys. Res., 102, 21493-21514, 1997b.

Figure Captions

Figure 1 A cartoon showing the path of irreducible parcels to the sample point. Two parcel paths are indicated by arrows, the filled circles indicate the parcel trace gas amounts. The color fill indicates the amount of N_2O in each parcel with darker color indicating a higher amount. The average path (average of many parcel paths) for parcels with the same age is shown by the dotted line. The background shows the loss rate (years^{-1}) for N_2O. The cartoon illustrates the situation where two parcels having, the same transit time to the sample point, nonetheless arrive with different amounts of N_2O. The horizontal lines indicate the tropopause.

Figure 2. The age spectrum and the tracer spectrum are compared for tracers with different lifetimes in years. The upper figure shows the age spectrum using HP's analytical model (Eq. 8), $K = 3.1 m^2/s$, $H = 7 km$, $z = 50 km$. The lower figure shows the corresponding tracer spectrum for trace gases with different lifetimes, β^{-1}, in Eq. (9). The vertical lines show the first moment of each distribution. In the upper figure, the first moment is the age-of-air, while in the lower figure the first moments are the mixing ratios for the sample with the assumed bottom boundary value of 1.0.

Figure 3. (Part a) Back trajectories positions from a regular array of 2001 starting points in a 1 km by 1° latitude grid box at 35°S latitude and 30km (small gray square). The parcel positions are plotted every 3.6 days and appear as a cloud of points surrounding the average path (white line). (Part b) The age spectrum for the grid box. The age for each parcel is the time required for the parcel to descend to 2 km. The age-of air or mean age is shown at the top of the figure.

Figure 4. (Left) Age-of-air for the 2D model computed using the Eulerian method. (Middle) Age-of-air computed using back trajectories. The age spectrum is computed using 400 parcels contained within a 1 km by 1° grid box centered at each of the 2D model grid points (see Fig. 6a). The age of air is then computed using from the spectrum. Random mixing is included (see text). (Right) Age-of-air computed from back trajectories using a uniform 2 km by 2° grid over the domain. Random mixing is not included.

Figure 5. (Part a) A scatter plot of N_2O verses age for the 2001 parcels shown in Figure 3. (Part b) The normalized N_2O tracer spectrum with the mean value indicated on the figure. The N_2O tracer amount is divided by the tropopause value. (Part c) A comparison of tracer fraction verses age for N_2O. Crosses indicate the average tracer fraction computed by integrating all the parcel back trajectories with the same age. Each parcel fraction is shown as a small dot. The filled circles show the results obtained from using APA for each age bin. (Part d) The age PDF (thin line) multiplied by the tracer fraction for each age (thick dashed line) shown in Part c. The thick solid line shows the results using APA. The two thick lines lie nearly on top of each other.

Figure 6.(Part a) The N_2O distribution for each grid box computed by integrating over each path and using the annually averaged loss rate from the 2D model. Grid box positions are shown on the figure. (Part b) The N_2O distribution computed using APA. (Part c) Difference between Parts b and c. (Part d) Plot of sample age-of-air verses N_2O amount for all the sample boxes shown in Part a.

Figure 7. A cartoon that shows our interpretation of trace gas measurements. In the upper panel an aircraft collects samples of air indicated by colored dots. The green lines are equal age-of-air contours, or isochrons; the blue lines are constant potential surfaces or isentropes. The color of the dot indicates the age-of-air with blue indicating young air and

red indicating old air. The upper-middle panel shows the sample values of trace gases A and B plotted against each other. The data fit is the light blue line. In the lower-middle panels the age spectrum, G(t) is plotted for two of the samples. In the bottom panel, the age spectrum for the old and young samples are seen to form from the weighting of points on the single path photochemistry curve. As irreducible parcels move through the stratosphere, they travel down the single path photochemistry curve as their photochemical exposure increases.

Figure 8. (Top) The solid line shows N_2O versus CFC-11 using each of the chemical trajectory values. The mixing of the Lagrangian points according to the age spectrum (10) form the circles. The numbers next to each circle indicate the age-of-air. The dotted line is the PK-limit curve defined using the global lifetime of the two tracers from the 2D model and Eq (17). (Bottom) The same diagram using the log of the mixing ratio.

Figure 9. As in Figure 8, the Lagrangian points (red line), and data from samples within 10° by 2 km region centered on the 2D model grid (crosses). ATMOS measurements (pink circles) from the ATLAS 1-3 missions are also shown. The PK limit for the 2D model is the dashed line (see Fig. 8). The 2D model data falls between the single path photochemistry limit and the PK limit as expected. The ATMOS data is not constrained to tropospheric values of N_2O or CFC-11 so may fall above the PK limit curve.

Parcel Trajectories in the Stratosphere

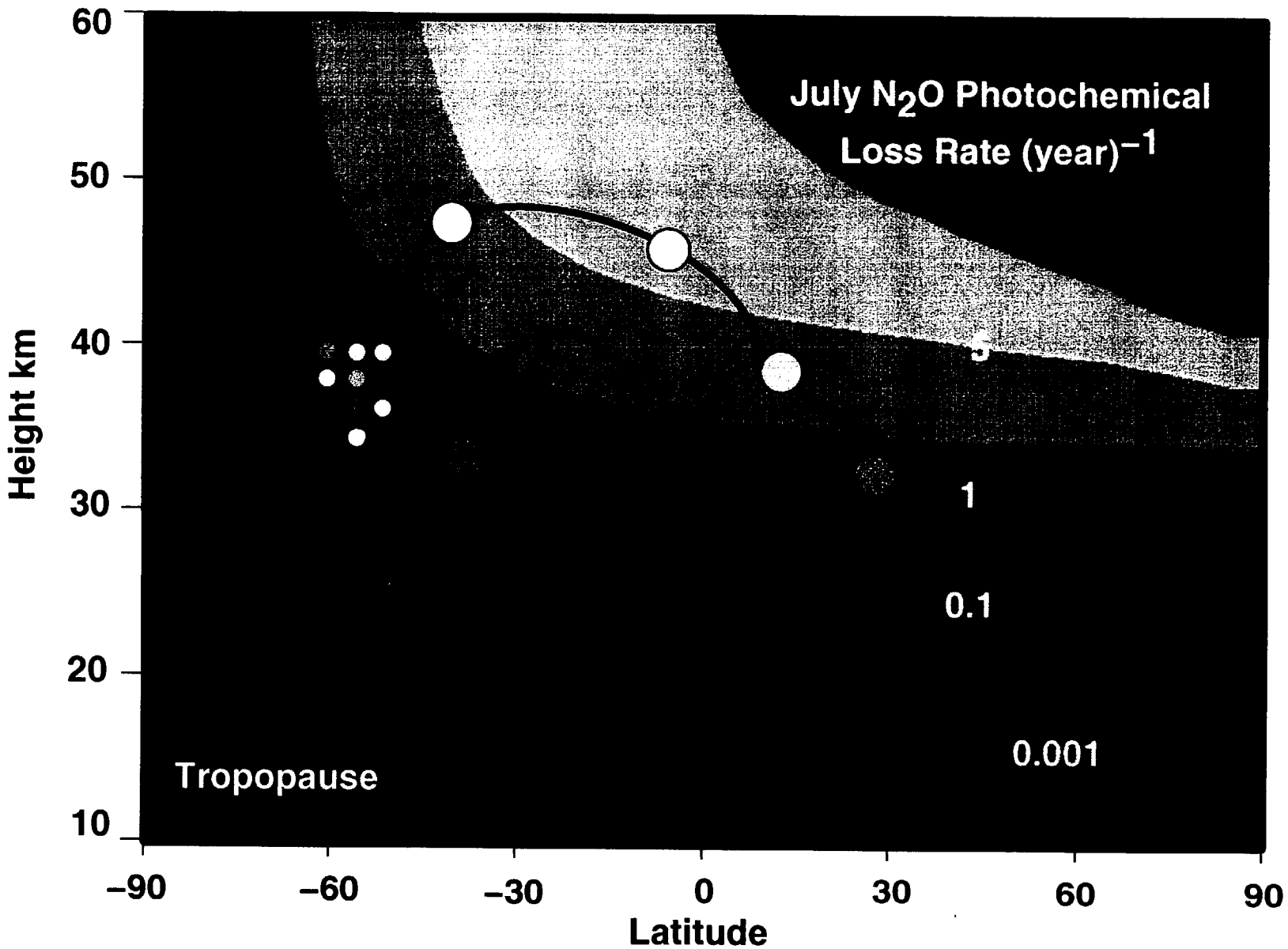

Fig. 1

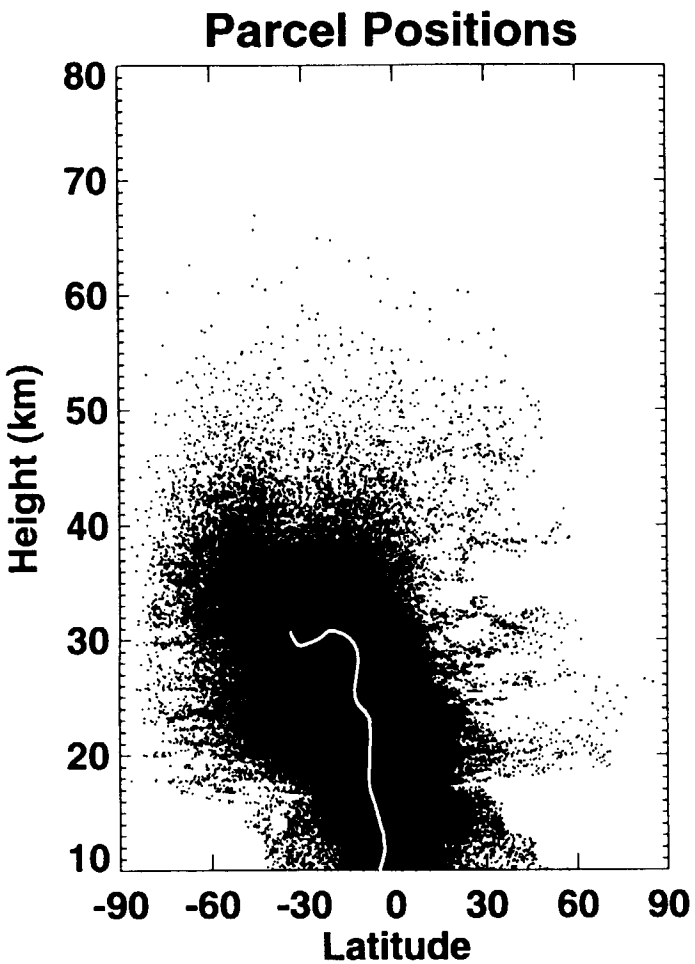
Parcel Positions
Height (km)
80
70
60
50
40
30
20
10
-90
-60
-30
0
30
60
90
Latitude

3a

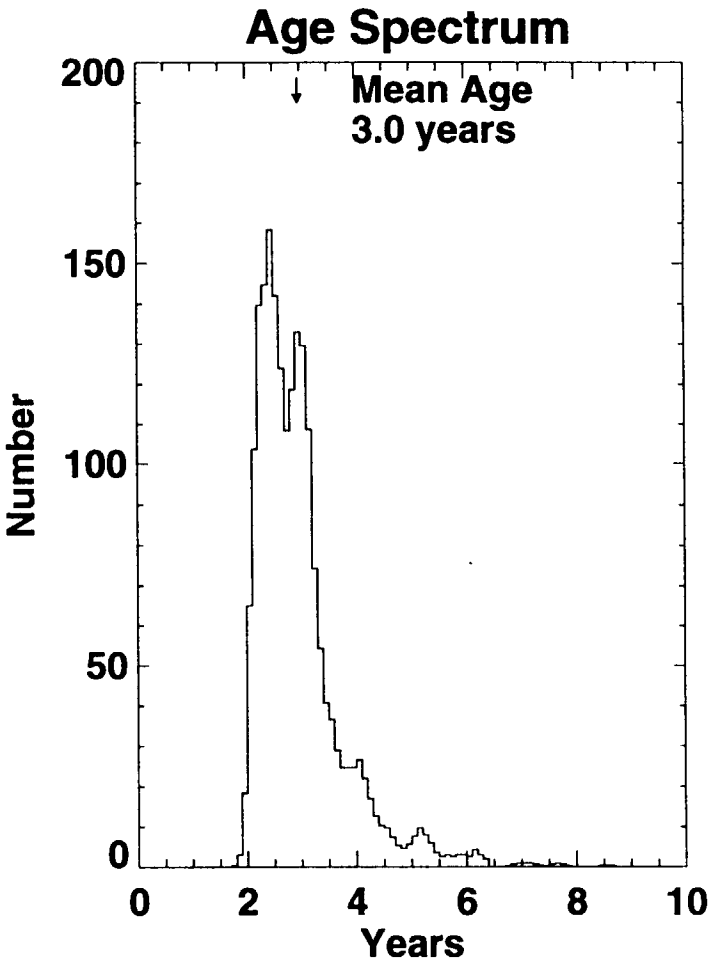
Age Spectrum
Mean Age
3.0 years
Number
200
150
100
50
0
0
2
4
6
8
10
Years

3b

Fig 2

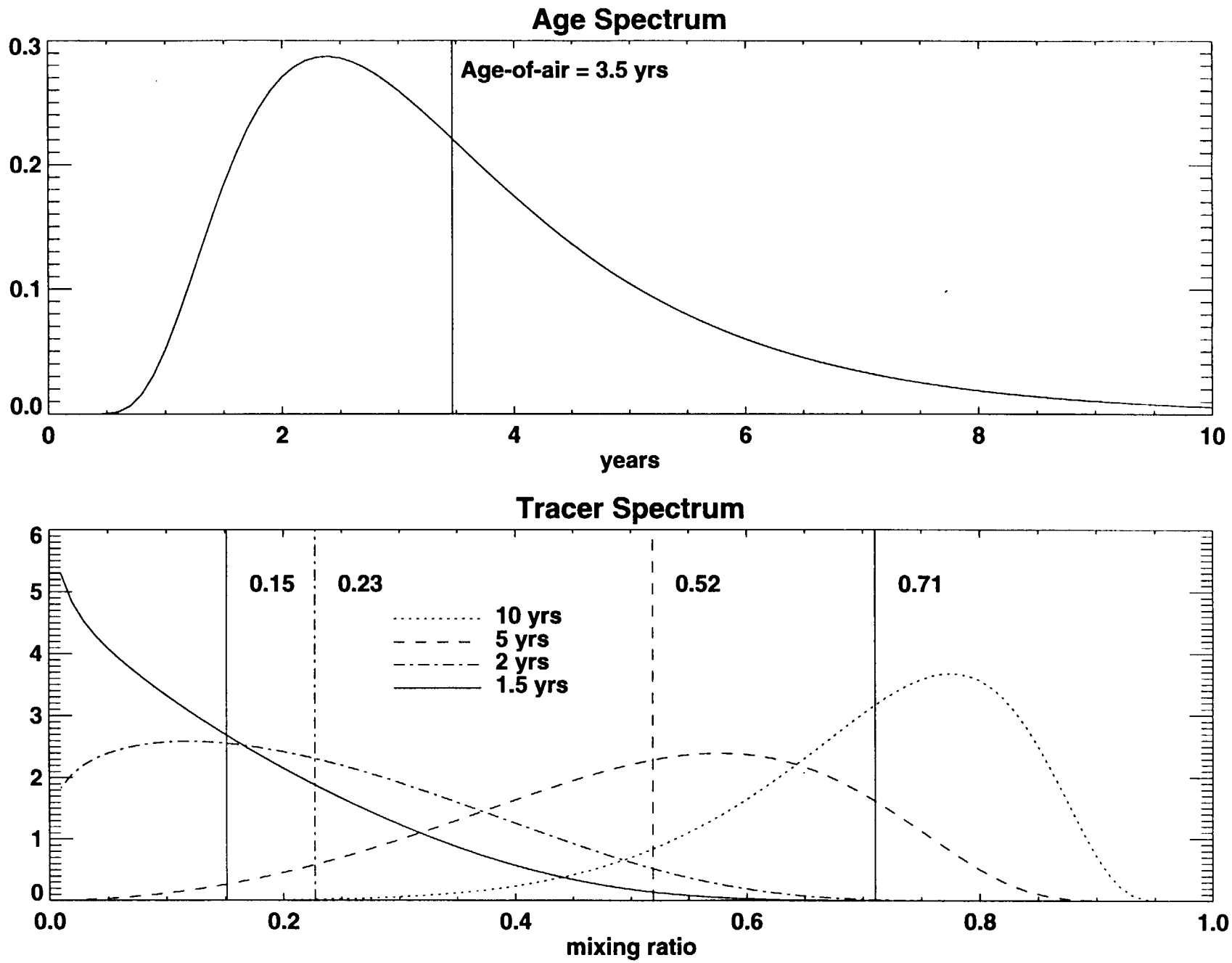
Age Spectrum
Age-of-air = 3.5 yrs
0.3
0.2
0.1
0.0
0
2
4
6
8
10
years
Tracer Spectrum
0.15
0.23
0.52
0.71
10 yrs
5 yrs
2 yrs
1.5 yrs
6
5
4
3
2
1
0
0.0
0.2
0.4
0.6
0.8
1.0
mixing ratio

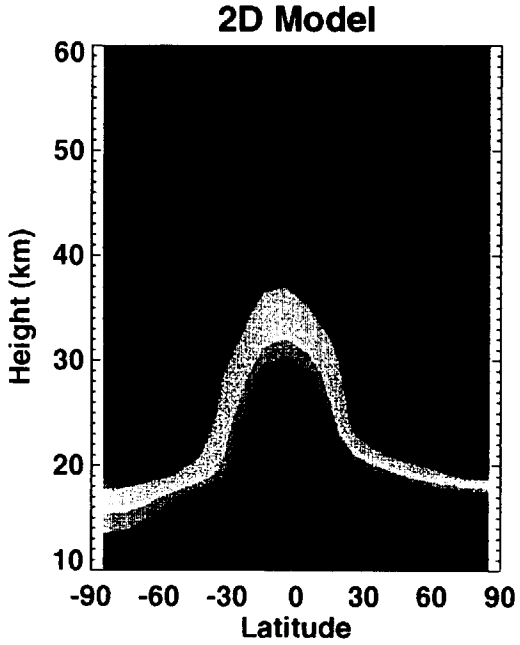
2D Model
Height (km)
60
50
40
30
20
10
-90 -60 -30 0 30 60 90
Latitude

4a

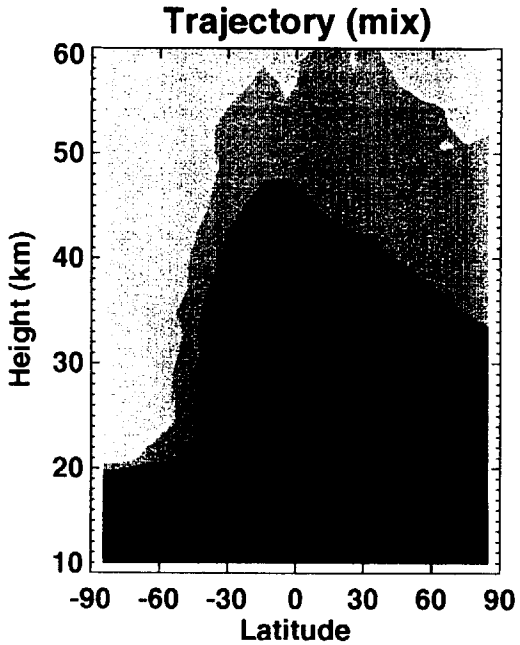
Trajectory (mix)
Height (km)
60
50
40
30
20
10
-90 -60 -30 0 30 60 90
Latitude

4b

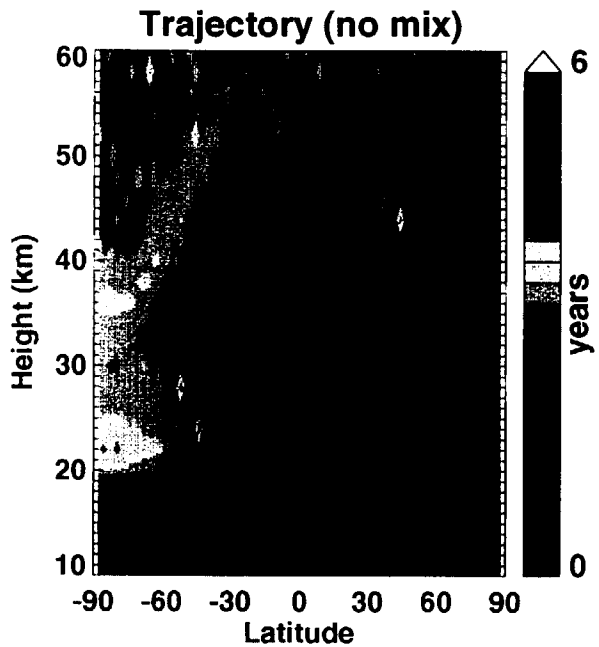
Trajectory (no mix)
Height (km)
60
50
40
30
20
10
-90 -60 -30 0 30 60 90
Latitude
6
years
0

4c

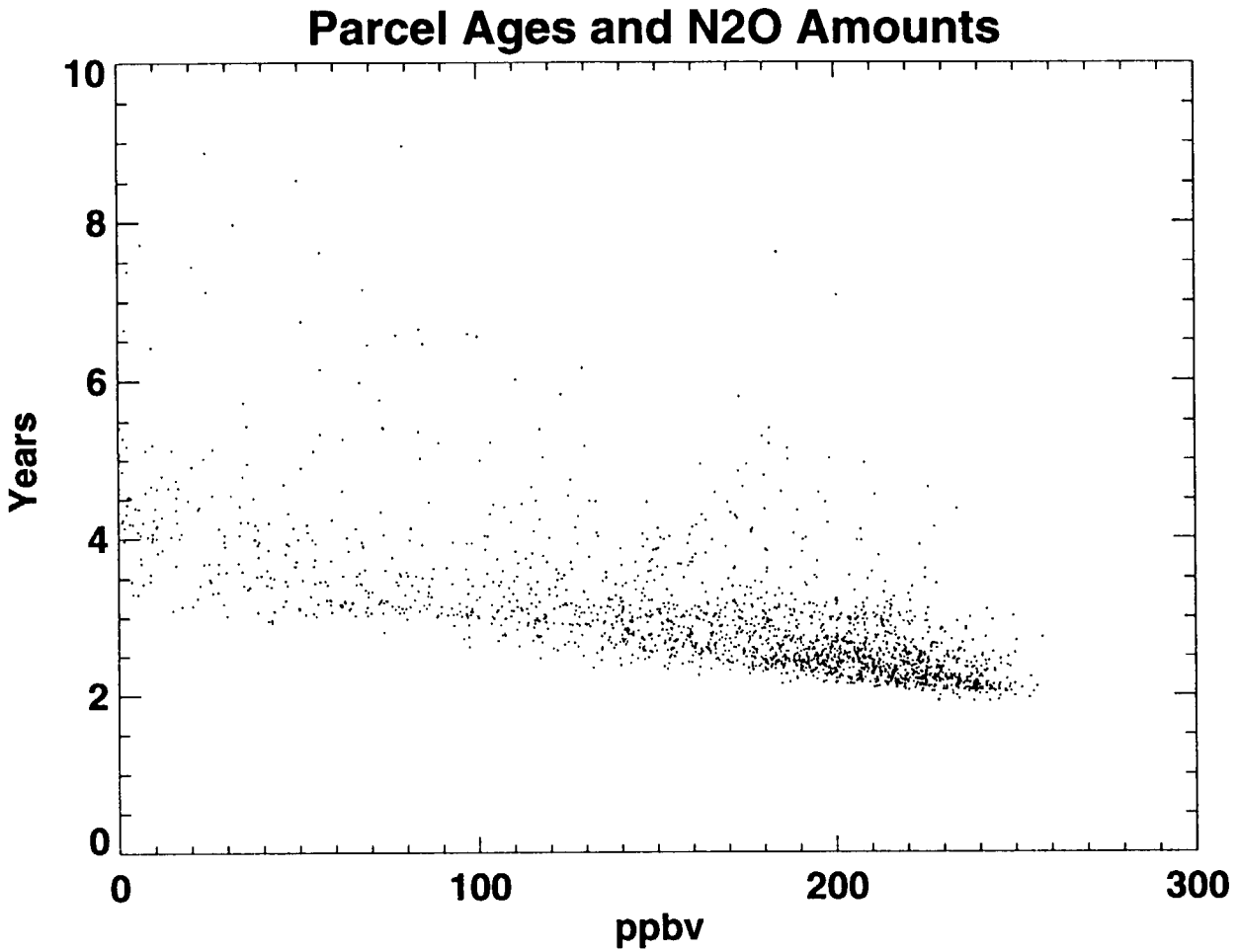

Fig. 5a

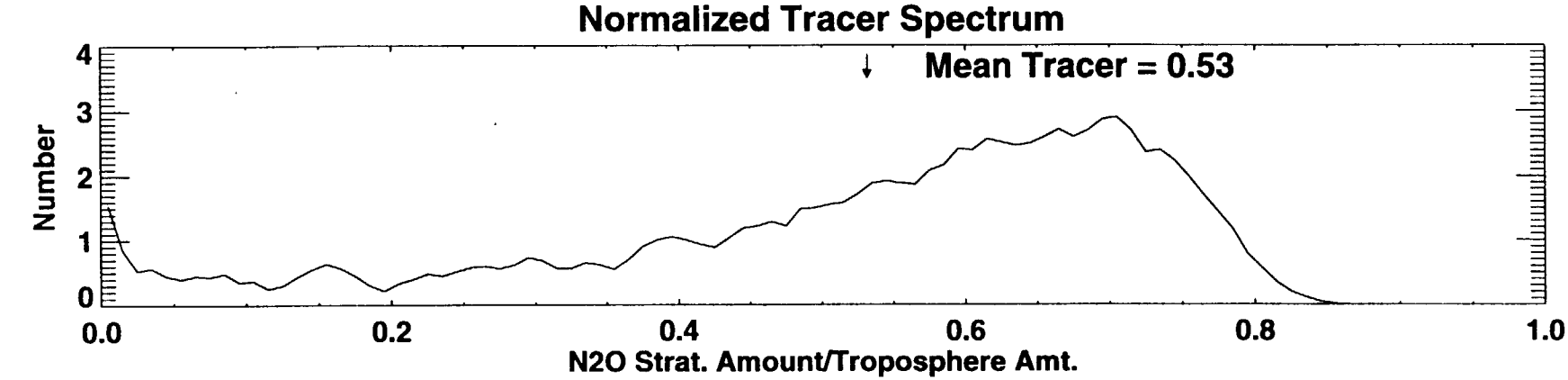
Normalized Tracer Spectrum
Mean Tracer = 0.53
Number
0
1
2
3
4
0.0
0.2
0.4
0.6
0.8
1.0
N2O Strat. Amount/Troposphere Amt.

5b

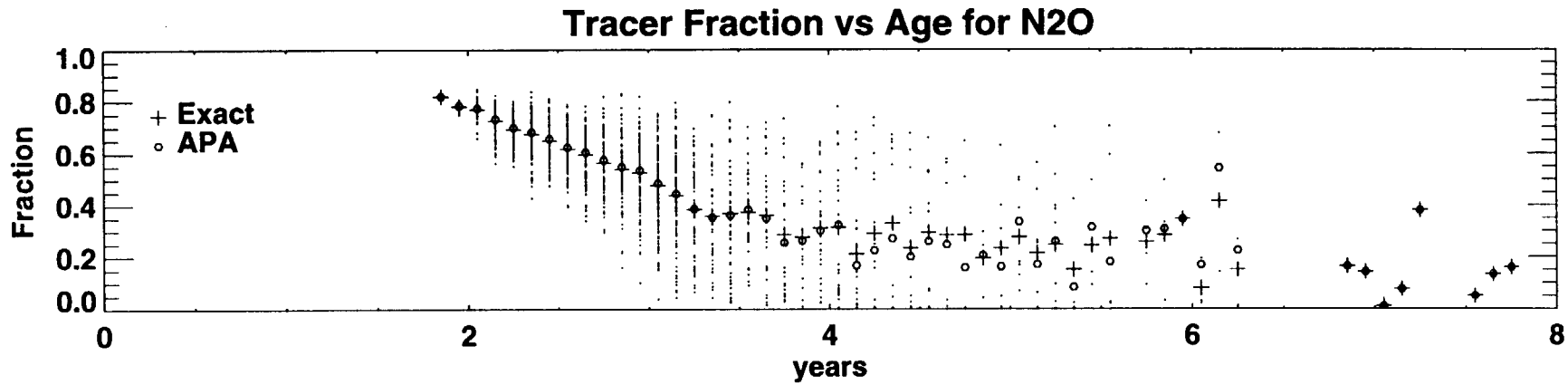
Tracer Fraction vs Age for N2O
Exact
APA
Fraction
0.0
0.2
0.4
0.6
0.8
1.0
0
2
4
6
8
years

5c

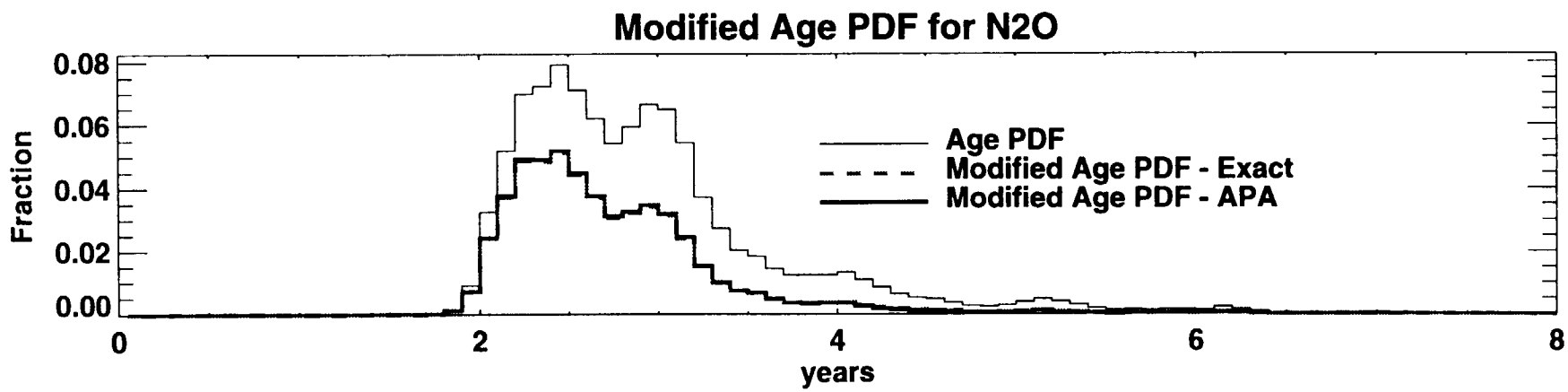
Modified Age PDF for N2O
Age PDF
Modified Age PDF - Exact
Modified Age PDF - APA
Fraction
0.00
0.02
0.04
0.06
0.08
0
2
4
6
8
years

5d

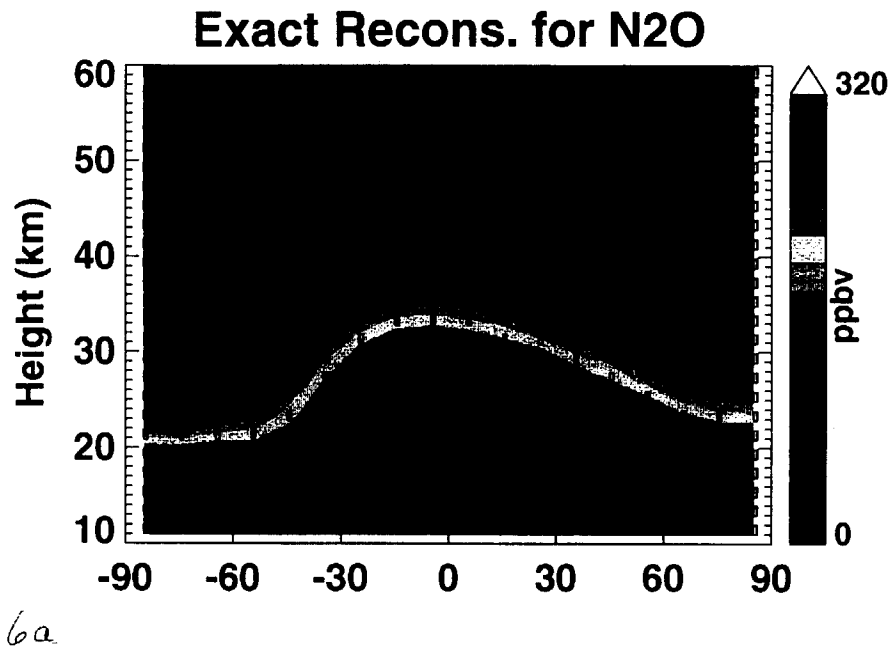
Exact Recons. for N2O
Height (km)
60
50
40
30
20
10
-90
-60
-30
0
30
60
90
320
ppbv
0

6a

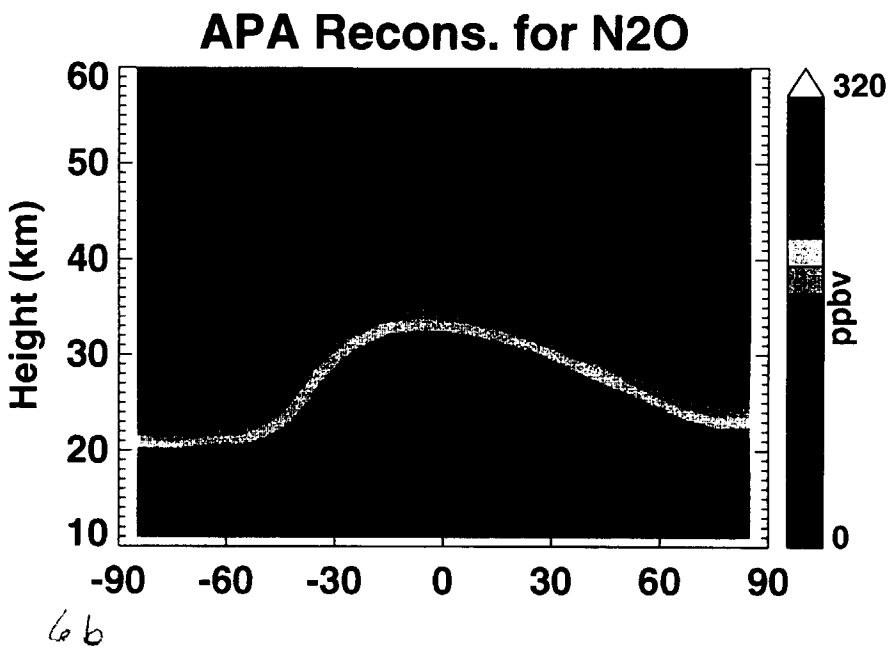
APA Recons. for N2O
Height (km)
60
50
40
30
20
10
-90
-60
-30
0
30
60
90
320
ppbv
0

6b

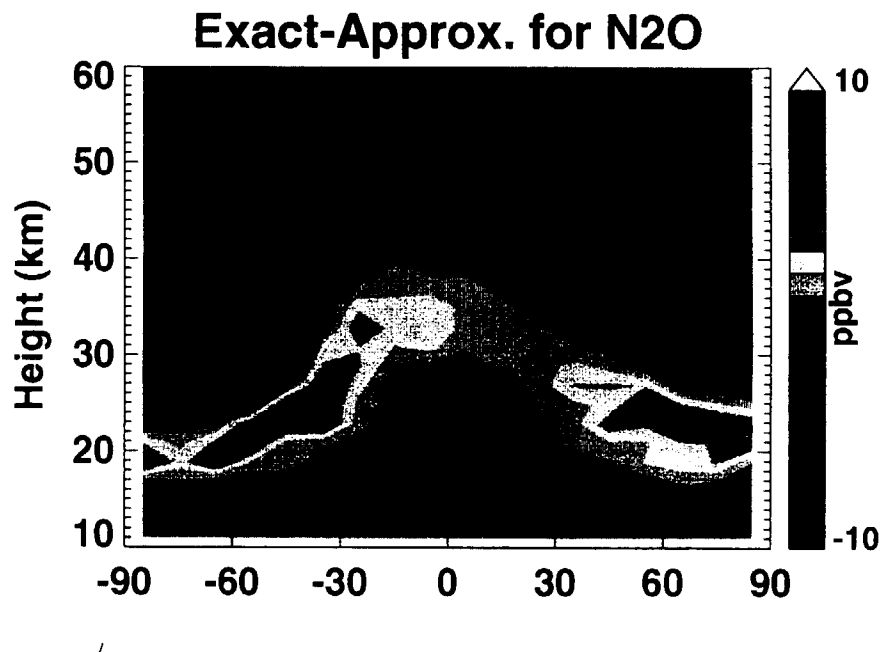
Exact-Approx. for N2O
Height (km)
60
50
40
30
20
10
-90
-60
-30
0
30
60
90
10
ppbv
-10

6c

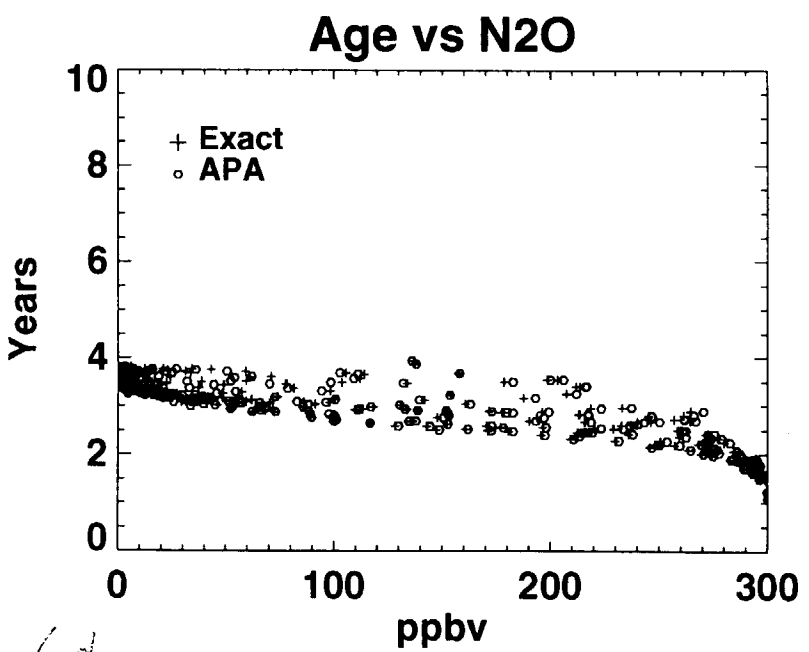
Age vs N2O
Years
10
8
6
4
2
0
+ Exact
o APA
0
100
200
300
ppbv

6d

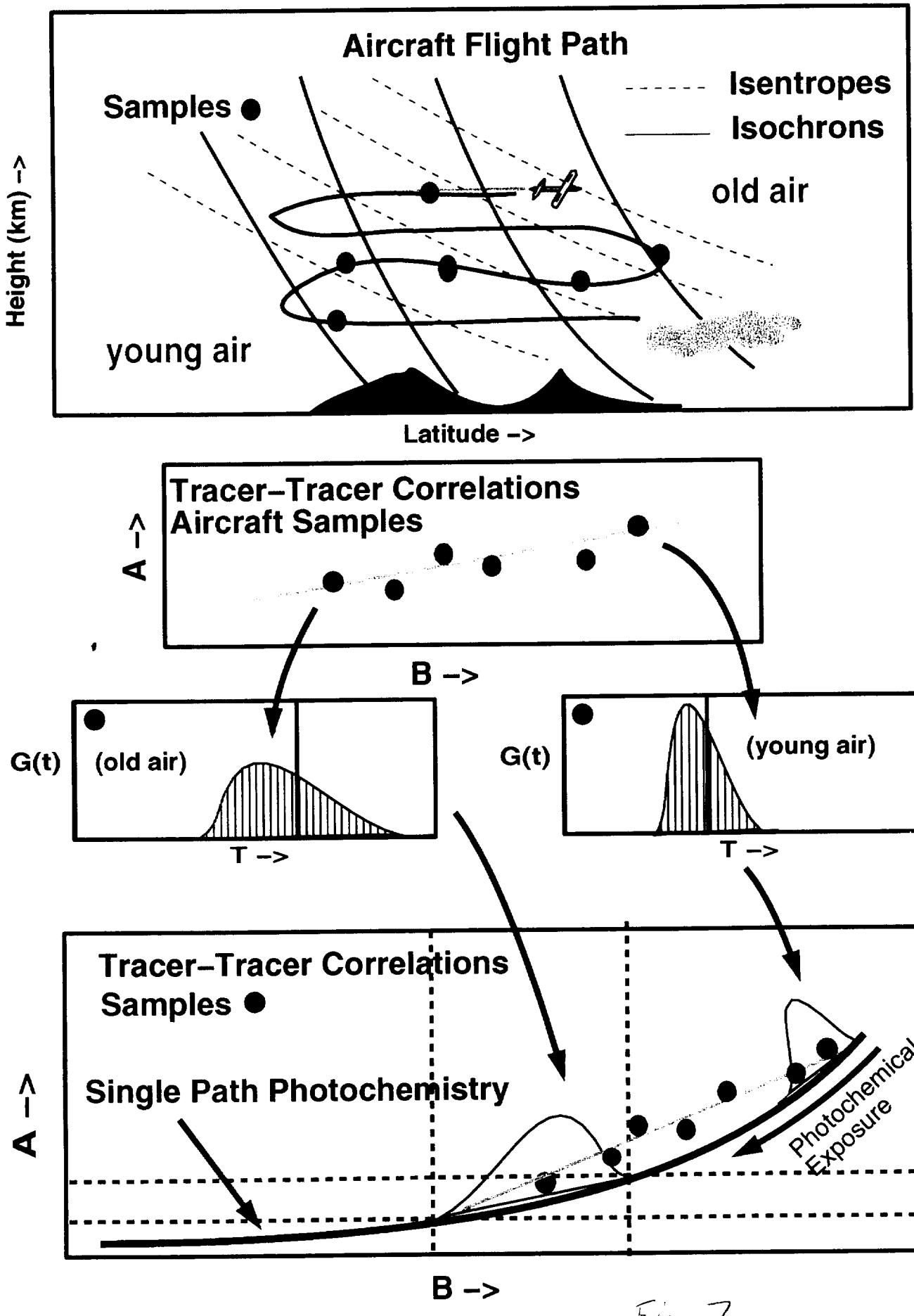
Aircraft Flight Path
Samples
Isentropes
Isochrons
old air
young air
Height (km) ->
Latitude ->
Tracer–Tracer Correlations
Aircraft Samples
A ->
B ->
G(t)
(old air)
T ->
G(t)
(young air)
T ->
Tracer–Tracer Correlations
Samples
Single Path Photochemistry
A ->
Photochemical Exposure
B ->

Fig. 7

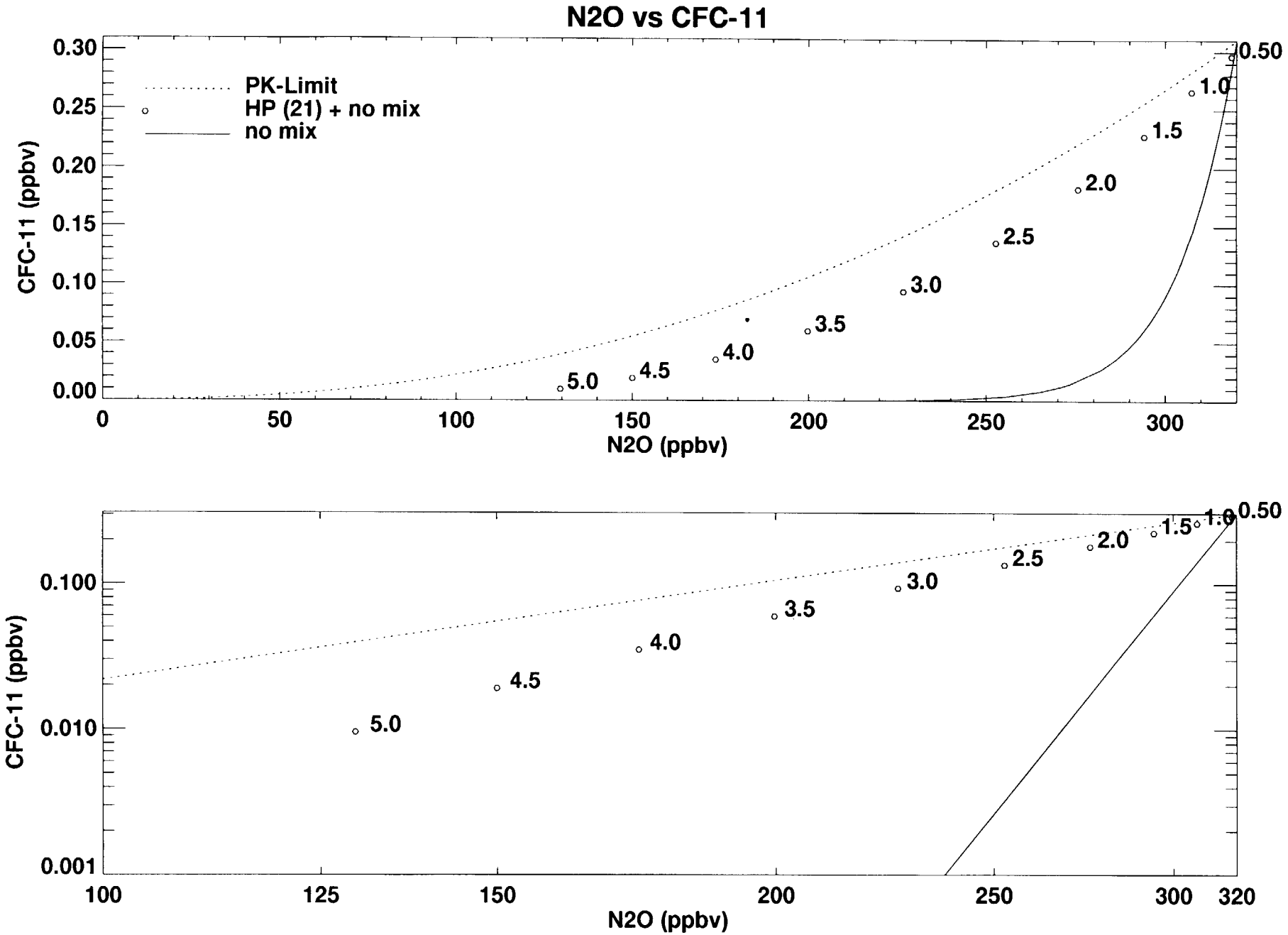
N2O vs CFC-11
PK-Limit
HP (21) + no mix
no mix
CFC-11 (ppbv)
N2O (ppbv)
0.30
0.25
0.20
0.15
0.10
0.05
0.00
0
50
100
150
200
250
300
0.50
1.0
1.5
2.0
2.5
3.0
3.5
4.0
4.5
5.0
0.100
0.010
0.001
100
125
150
200
250
300
320

8

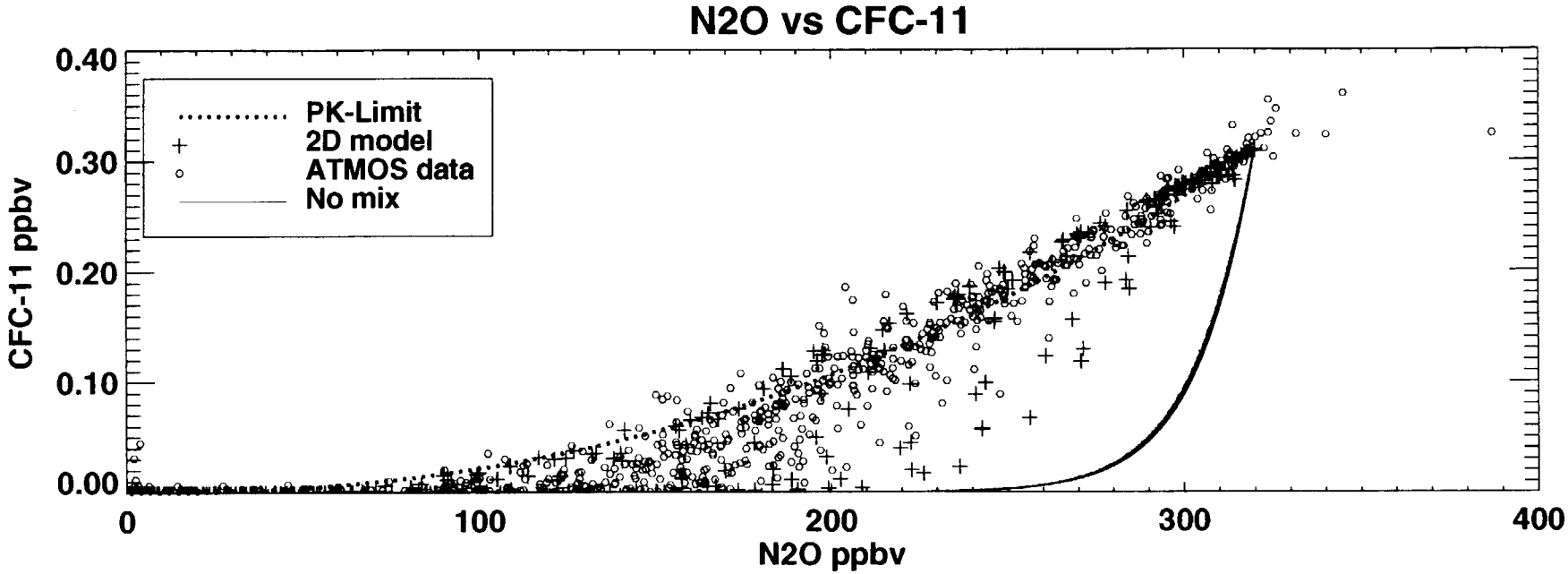
N2O vs CFC-11
PK-Limit
2D model
ATMOS data
No mix
CFC-11 ppbv
0.40
0.30
0.20
0.10
0.00
0
100
200
300
400
N2O ppbv

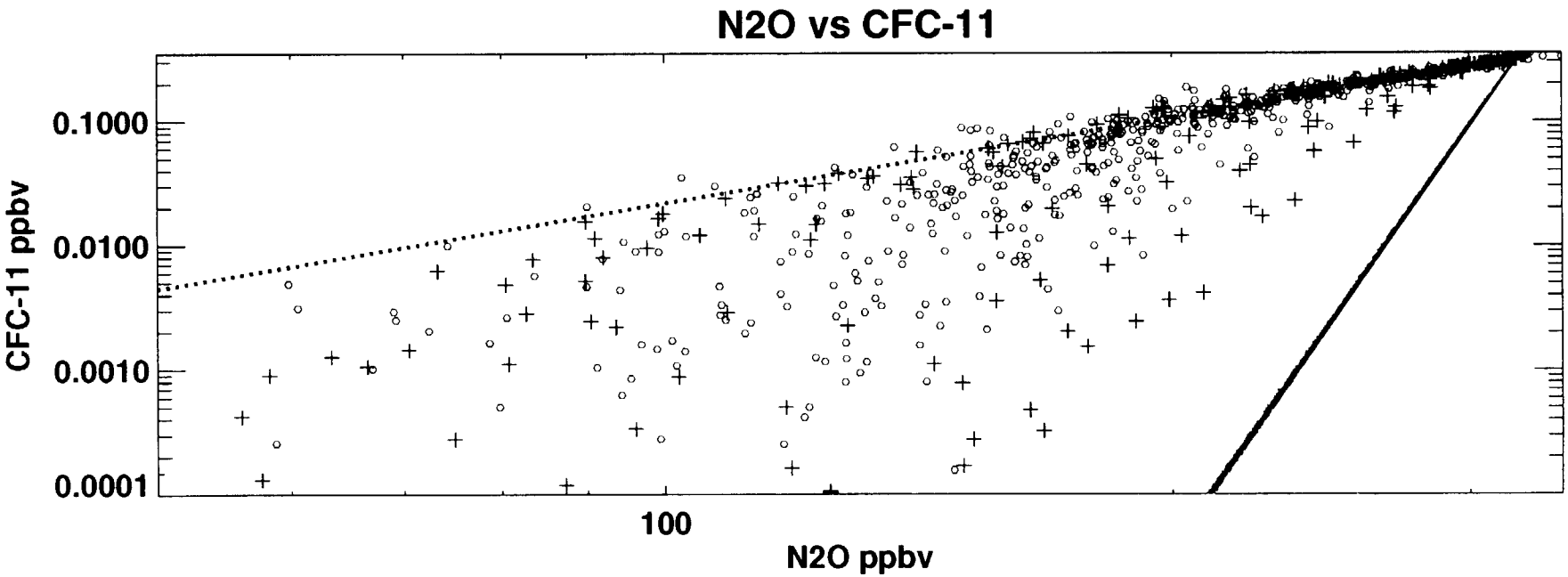
N2O vs CFC-11
CFC-11 ppbv
0.1000
0.0100
0.0010
0.0001
100
N2O ppbv

Parcel Trajectories in the Stratosphere